JACS
JOURNAL OF THE AMERICAN CHEMICAL SOCIETY
Article
pubs.acs.org/JACS

Polymer Triplet Energy Levels Need Not Limit Photocurrent Collection in Organic Solar Cells

Cody W. Schlenker,[†] Kung-Shih Chen,[‡] Hin-Lap Yip,[‡] Chang-Zhi Li,[‡] Liam R. Bradshaw,[†] Stefan T. Ochsenbein,[†,§] Feizhi Ding,[†] Xiaosong S. Li,[†] Daniel R. Gamelin,[†] Alex K.-Y. Jen,[‡] and David S. Ginger*[,†]

[†]Department of Chemistry, University of Washington, Seattle, Washington 98195-1700, United States

[‡]Department of Materials Science & Engineering, University of Washington, Seattle, Washington 98195-2120, United States

Supporting Information

ABSTRACT: We study charge recombination via triplet excited states in donor/acceptor organic solar cells and find that, contrary to intuition, high internal quantum efficiency (IQE) can be obtained in polymer/fullerene blend devices even when the polymer triplet state is significantly lower in energy than the intermolecular charge transfer (CT) state. Our model donor system comprises the copolymer PIDT-PhanQ: poly(indacenodithiophene-co-phenanthro[9,10-b]-quinoxaline), which when blended with phenyl-C_{71}-butyric acid methyl ester ($PC_{71}BM$) is capable of achieving power conversion efficiencies of 6.0% and IQE ≈ 90%, despite the fact that the polymer triplet state lies 300 meV below the interfacial CT state. However, as we push the open circuit voltage (V_{OC}) higher by tailoring the fullerene reduction potential, we observe signatures of a new recombination loss process near V_{OC} = 1.0 V that we do not observe for PCBM-based devices. Using photoinduced absorption and photoluminescence spectroscopy, we show that a new recombination path opens via the fullerene triplet manifold as the energy of the lowest CT state approaches the energy of the fullerene triplet. This pathway appears active even in cases where direct recombination via the polymer triplet remains thermodynamically accessible. These results suggest that kinetics, as opposed to thermodynamics, can dominate recombination via triplet excitons in these blends and that optimization of charge separation and kinetic suppression of charge recombination may be fruitful paths for the next generation of panchromatic organic solar cell materials with high V_{OC} and J_{SC}.

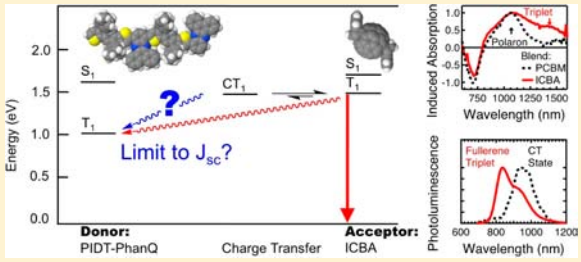

INTRODUCTION

Although significant progress[1−3] has been made to increase the power conversion efficiency of organic solar cells (e.g., η_P = 10.6% for tandem cell architectures),[4] the molecular design rules for achieving efficient systems are still unclear. General principles such as the importance of maximizing open circuit voltage (V_{OC}) by minimizing energy losses associated with exciton dissociation are widely recognized, yet discussions of the fundamental limits that might be realistically achieved are largely empirical.[5,6] For instance, both Veldman et al.[7] and Faist et al.[8] have argued that the maximum V_{OC} should be equal to the optical gap (E_{opt}/q_e) minus ∼0.60−0.66 V. Others have shown that V_{OC} correlates well with the energy of the Coulombically bound interfacial charge transfer (CT) state between the hole on the donor and the electron on the acceptor,[9−12] an energy that can be altered by controlling the reduction potential of the acceptor and the oxidation potential of the donor. However, pinpointing the mechanistic details of the loss processes that limit η_P is of critical importance to improving organic solar cell performance.

To this end, the roles of both triplet states[13−16] and interfacial charge transfer[7,10,17−19] (CT) states as mediators of recombination losses have been highlighted by a number of authors. In particular, charge recombination via the donor triplet[20] has been identified as a process that can limit attainable J_{SC} whenever the energy of the interfacial CT state is raised above that of the donor triplet state.[7,15,19−23]

Here, we study losses via the triplet manifold and show that efficient photocurrent collection at short circuit, as well as reasonable fill factors, can be maintained even in cases where the lowest interfacial CT state is several hundred meV higher in energy than the triplet state of the donor polymer PIDT-PhanQ (a copolymer of indacenodithiophene and phenanthro-[9,10-b]quinoxaline derivatives shown in Figure 1a) when this donor material is blended with phenyl-C_{71}-butyric acid methyl ester ($PC_{71}BM$). As we alter the fullerene reduction potential to raise V_{OC}, we ultimately do observe increased recombination loss and polymer triplet formation, but it appears that the fullerene triplet serves as the key intermediate when the CT state and the fullerene triplet state become nearly degenerate in energy. These observations point toward the importance of device optimization strategies that transcend simple energy level matching, such as the design of molecular motifs for

Received: June 22, 2012
Published: November 5, 2012

   dx.doi.org/10.1021/ja306110b | J. Am. Chem. Soc. 2012, 134, 19661−19668

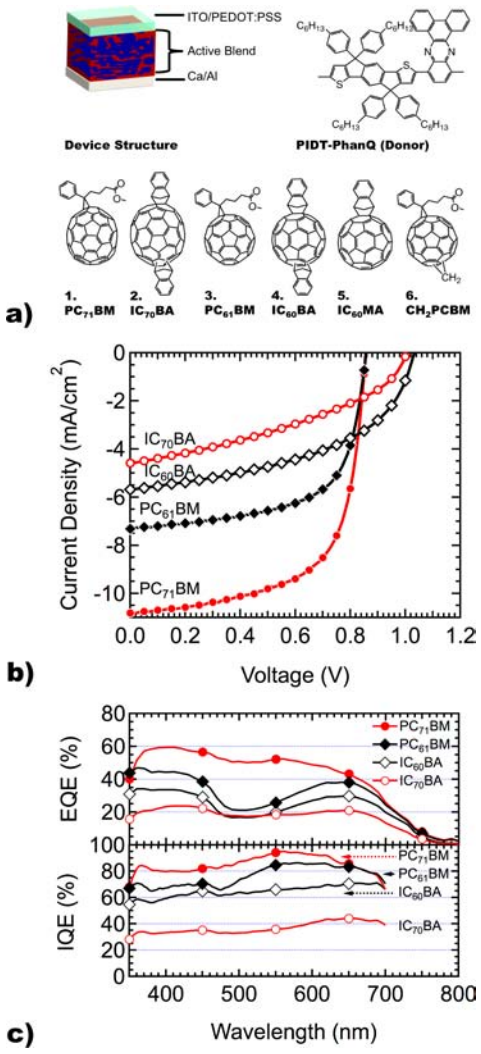

Figure 1. (a) Schematic depiction of the solar cell device structure employed here, consisting of a blended polymer:fullerene active layer with PIDT-PhanQ as the donor. Fullerene acceptors **1**–**6** used in this study are also depicted. (b) Photocurrent density as a function of voltage for the device structure in (a) using fullerenes **1**–**4** as acceptor materials, measured under simulated AM1.5G solar illumination at 1 kWm^{-2}. (c) External (upper panel) and internal (lower panel) quantum efficiency for devices in (b).

kinetic optimization of charge separation efficiency and suppressed recombination.

MATERIALS AND METHODS

Indene-fullerene *bis*-adducts[24−26] and adduct **5**[27] were synthesized according to literature procedures. Methano-$PC_{61}BM$ **6** was synthesized as described previously,[28] as was PIDT-PhanQ.[29] $PC_{71}BM$ of >98% purity (ADS, American Dye Source, Quebec, Canada), poly(3,4-ethylenedioxy-thiophene):poly(styrene sulfonate) (PEDOT:PSS, Baytron P VP AI 4083, H. C. Stark. Chemicals) were purchased from commercial sources and used as received.

Device and Spectroscopic Sample Fabrication. PIDT-PhanQ:fullerene mixtures (1:3 w/w) were dissolved in 1,2-dichlorbenzene (Aldrich) and stirred on a hot plate at 90 °C overnight under inert atmosphere. We found this blending ratio to yield optimal device performance (cf. Supporting Information Figure S10b). Solar cells were fabricated in the conventional geometry. ITO coated glass substrates (15 Ω per square) were solvent cleaned followed by oxygen plasma treatment for 30 s. PEDOT:PSS (50 nm) was spin-coated on clean ITO substrates and annealed at 140 °C in ambient, followed by spin-coating the active layers on PEDOT:PSS coated ITO from filtered (0.20 μm PTFE) PIDT-PhanQ:fullerene solutions. Thin film optical samples were prepared under identical conditions on clean glass substrates free of ITO or PEDOT:PSS.

Device Testing. Device *J*−*V* measurements were performed under a nitrogen atmosphere using a Keithley 2400 source meter. A KG5 filtered silicon photodiode, calibrated at the National Renewable Energy Laboratory (NREL), was used to calibrate the simulated solar illumination intensity (1 kWm^{-2}) from a 450 W xenon arc lamp (Oriel) equipped with an AM 1.5G filter. Spectral photocurrent was recorded in room atmosphere under monochromated illumination from a 450 W xenon lamp, unless otherwise noted. The incident beam was chopped with a mechanical chopper, and the photocurrent was recorded with a lock-in amplifier (Stanford Research Systems SR830) with EQE calculated based on measurements from an NREL calibrated silicon photodiode. Within the short time frame (less than 10 min) of our spectral photocurrent experiment we obtain EQE values that are nearly identical (less than 5% relative difference) to measurements performed on devices without aerobic exposure (cf. Supporting Information Figure S10).

Spectroscopic Characterization and Microscopy. All thin film photoluminescence measurements were performed on a home-built spectrometer using a Si/InGaAs two-color photodiode, frequency modulated illumination from a 455 nm LED (Luxeon), and standard lock-in techniques. Spectral correction was performed using a calibrated light source (OceanOptics). PL measurements in frozen anaerobic solution were performed at 80 K in a quartz EPR tube under illumination from a 375 nm diode laser (PicoQuant) and collected using a CCD camera (Princeton Instruments, Spec-10) following dispersion onto the grating of a monochromator. EPR measurements were performed on solid PIDT-PhanQ:fullerene solutions prepared in a quartz EPR tube by vacuum concentration from liquid *o*-DCB solutions identical to those used for PIA. LEPR measurements were performed on a Bruker E580 X-Band EPR Spectrometer at 120 K and the resulting LEPR signal plotted as the difference in microwave absorbance in the presence and absence of illumination from a 455 nm LED (Luxeon, 5W). PIA spectra were collected as previously described[30] using conventional lock-in detection methods[31] employing a 455 nm LED (Luxeon, 5W) excitation source modulated at 200 Hz unless otherwise specified. Measurements were performed in transmission mode on glass substrates in vacuum at room temperature or at low-temperature in a Janis continuous flow cryostat. The optical constants of the polymer:fullerene films were measured using a variable angle spectroscopic ellipsometer (J. A. Woollam Co. M-2000). Absorption in the active layer of each device was calculated using the transfer matrix approach outlined in the literature[32] to account for interference. The layer structure used to represent the device in the optical model comprised Glass/ITO(110 nm)/PEDOT:PSS(35 nm)/Active Layer (*X* nm)/Ca (20 nm)/Al (100 nm), where the active layer thickness, *X*, was determined by atomic force microscopy (AFM) for a representative active layer film cast onto a clean glass slide and assuming ca. 10 nm metal diffusion during electrode deposition.[33] Surface topography images were collected on a Veeco multimode AFM with a Nanoscope III controller.

RESULTS AND DISCUSSION

We chose to study recombination losses in indacenodithiophene-based[34−41] polymer devices, specifically PIDT-PhanQ:fullerene blends, because such devices have achieved both high efficiency and high V_{OC} (η_P = 6.0% and V_{OC} = 0.86 V)[29] and because they exhibit clean spectroscopic signatures that allow us to probe CT energies as well as charge and triplet populations optically (see below). We altered the energy of the blend CT state by changing the electron affinity of the acceptor upon replacing PCBM with each fullerene in the series of derivatives **1**–**6** shown in Figure 1a. We find the half wave reduction potentials for compounds **1**–**6**, respectively, to be −1.07, −1.26, −1.07, −1.24, −1.123 and −1.22 V vs ferrocene/

dx.doi.org/10.1021/ja306110b | J. Am. Chem. Soc. 2012, 134, 19661−19668

ferrocenium. These results are in agreement with literature reports, with PCBM derivatives having the least negative reduction potentials and both C_{60} and C_{70} indene-fullerene-*bis*-adducts (ICBA) having reduction potentials ca. 170−190 mV more negative than their PCBM counterparts.[25,26] Figure 1b compares the impact on J_{SC}, V_{OC}, and *FF* in the extreme cases of using either PCBM or ICBA acceptors. Previous reports of poly(3-hexylthiophene) (P3HT)[24−26] with ICBA have shown significant enhancements in V_{OC} values compared to PCBM blends, with J_{SC} being maintained in the ICBA-based device. Similar V_{OC} enhancements have been attributed to destabilization of the CT state when using fullerenes that are more difficult to reduce.[42,43] Figure 1b and Table 1 show that switching to ICBA also increases V_{OC} for our PIDT-PhanQ blends. The value of V_{OC} = 1.0 V for the ICBA blends is 140 mV larger than that for the PCBM-based devices (V_{OC} = 0.86 V). However, our devices exhibit a marked trade-off between J_{SC} and V_{OC}. This trade-off is in contrast to what has been observed for P3HT:ICBA devices compared to P3HT:PCBM but is consistent with reports from some other high-performance polymer/PCBM blends like the carbazole-based donor−acceptor polymer PCDTBT.[44]

Table 1. Performance Metrics for PIDT-PhanQ:fullerene Devices under Illumination[a]

Device[b]	J_{SC} (mA/cm^2)	V_{OC} (V)	*FF*	η_P (%)
$PC_{71}BM$	10.8	0.86	0.64	6.0
$PC_{61}BM$	7.30	0.86	0.63	4.0
$IC_{60}BA$	5.69	1.0	0.49	2.9
$IC_{70}BA$	4.60	1.0	0.39	1.8

[a]Simulated 1 sun (1 kWm^{-2}) AM1.5G. [b]Glass/ITO/PEDOT:PSS/PIDT-PhanQ:fullerene/Ca/Al, where fullerene denotes the acceptor material listed in the "Device" column.

Since the smaller η_P for both ICBA derivatives is due in part to substantial losses in J_{SC}, we examined both the external (EQE) and internal (IQE) quantum efficiencies for these devices. Figure 1c plots EQE and IQE values for these blends as a function of wavelength. The upper panel of Figure 1c shows that the trend in EQE coincides with the trend in J_{SC} ($PC_{71}BM$ > $PC_{61}BM$ > $IC_{60}BA$ > $IC_{70}BA$). The IQE values plotted in the lower panel of Figure 1c were determined using the transfer matrix approach to calculate the active layer absorption[32] from optical constants obtained by variable angle spectroscopic ellipsometry. Significantly, the IQE values for the PCBM derivatives are quite high, with the IQE for $PC_{71}BM$ exceeding 90% over much of the visible region.

These high IQE values underpin the strong device performance of the PIDT-PhanQ:fullerene system, and place these blends among the highest performing materials reported.[3,45,46] The IQE values for the ICBA-based devices are lower than for the PCBM devices, indicating that their lower J_{SC} cannot be attributed solely to diminished photon absorption. We believe the high IQEs, and the changes observed upon fullerene derivatization, are noteworthy given

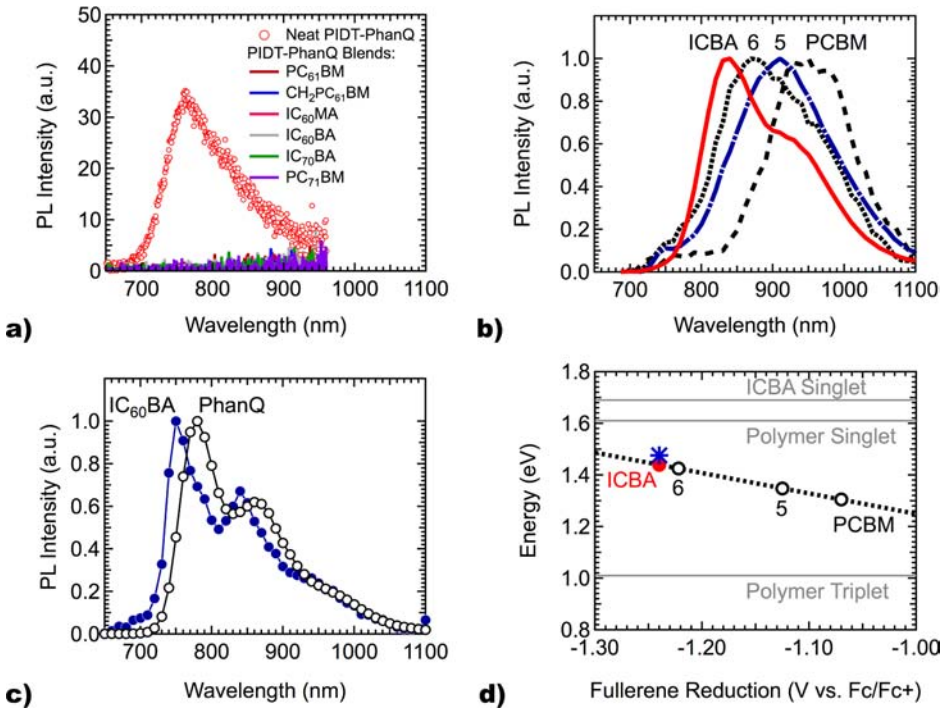

Figure 2. (a) Room temperature photoluminescence (PL) spectra of PIDT-PhanQ (red circles) with 17% fluorescence quantum yield. Fluorescence quenching is observed when PIDT-PhanQ is blended (solid traces) with any of fullerenes **1**−**6** in Figure 1a. (b) Normalized PL spectra measured at 80 K for each fullerene **3**−**6** in Figure 1a blended with PIDT-PhanQ. (c) Normalized PL measured at 80 K for neat PIDT-PhanQ (unfilled black circles) or $IC_{60}BA$ dispersed in polystyrene (filled blue circles). (d) Energy of the charge transfer (CT) state emission peak (unfilled circles) for blends in (b) as a function of fullerene reduction potential and least-squares fit (dashed black line with respective slope and intercept of −0.79 eV/V and 0.46 eV) used to estimate the CT state energy for the PIDT-PhanQ:$IC_{60}BA$ (filled red circle). The triplet energy of $IC_{60}BA$, obtained from the fullerene phosphorescence peak maximum, is also included (blue asterisk), along with exciton energies (solid gray lines) for both blend components. All spectra were collected using 455 nm excitation. Note that the energy of the triplet emission peak maxima for C_{60} derivatives related to $PC_{61}BM$ (E_T = 1.50 eV) that have been reported in the literature[7,48] are very close to the $IC_{60}BA$ triplet emission energy that we measure (E_T = 1.48 eV).

dx.doi.org/10.1021/ja306110b | J. Am. Chem. Soc. 2012, 134, 19661−19668

the driving forces for recombination to form triplet excitons in these blends. Below, we explore the limits of the PIDT-PhanQ:fullerene system in more detail by modulating the energy of the CT state and correlating the resulting device performance with spectroscopic signatures for various recombination pathways. To investigate charge recombination pathways in our ICBA OPVs we employed photoluminescence (PL), photoinduced absorption (PIA) spectroscopy, and light-induced EPR (LEPR) spectroscopies. We focus our discussion on the optical spectroscopy of the C_{60} blends exclusively because the PIA spectra of the C_{70} blends are more complex, due to the overlap of the C_{70} and polymer excited state features (Supporting Information Figure S1).

Figure 2a compares the room temperature photoluminescence spectra for the pure PIDT-PhanQ polymer and blends of the polymer with each of the fullerenes **1**−**6** (Figure 1a). The photoluminescence of the pristine polymer is completely quenched by every fullerene that we have studied, indicating that a lack of exciton quenching is not responsible for the decreased photocurrents observed in the ICBA blends. The near-complete quenching of the native polymer photoluminescence in the PIDT-PhanQ:fullerene blends is advantageous because it allows us to determine the energies of the relevant CT states directly from their photoluminescence peaks.

Figure 2b shows the photoluminescence from each blend measured at 80 K, and Figure 2c shows the photoluminescence from the neat polymer and from ICBA dispersed in polystyrene, also measured at 80 K. In all cases new emission bands appear in the blends (Figure 2b) that are distinct from the fluorescence of the individual components (Figure 2c), while the spectrum of the pure fullerene is consistent with previous reports of fullerene fluorescence.[47,48] The new peaks in the blends appear at lower energy than the S_1−S_0 emission from either the polymer or the fullerene and we assign these peaks (except in the case of PIDT-PhanQ:ICBA) as emission from intermolecular CT states based on two observations. First, with the notable exception of the PIDT-PhanQ:ICBA blend, these peaks exhibit unstructured PL bands characteristic of intermolecular CT emission.[49,50] Second, excluding the structured peak observed in the PIDT-PhanQ:ICBA blend, the peak positions of these CT bands shift linearly with the fullerene half-wave reduction potentials with slope and intercept of −0.79 eV/V and 0.46 eV, respectively (Figure 2d). Similar CT state emission has been observed for many donor/acceptor heterojunctions,[22,51−55] with linear correlations between E_{CT} and V_{OC} giving slopes near unity, but CT emission from an entire series of structurally related fullerene acceptors is uncommon.[8] Figure 2d compares the relative energies of the relaxed CT states in these blends with the energies of the singlet and triplet excited states for both the polymer and fullerene. We determined the relative CT state energies based on the PL emission peak maxima (Figure 2b), following the conventions of Tvingstedt et al.[53] and Veldman et al.[7] The relative energies of the S_1 states for the polymer and fullerene and the fullerene T_1 state were taken as the PL peak maxima (Figure 2c and Figure 4b).[56] We place an upper limit on the polymer T_1 energy at ca. 1.01 eV, based on predictions made using quantum chemical computational methods (Supporting Information Table S1) and in accord with reported exchange energies for other conjugated polymers.[57−60]

Notably, the energies of the CT states in all of the PIDT-PhanQ:fullerene blends we studied lie well above the polymer T_1 state. Even in the PIDT-PhanQ:PC_{71}BM blend with one of the lowest CT state energies (E_{CT} = 1.31 eV, Supporting Information Figure S2a) the CT state is at least 300 meV above the T_1 state of PIDT-PhanQ. Nevertheless, this blend converts absorbed photons to photocurrent with an internal quantum efficiency of over 90% across most of the visible. Previous work has suggested that the relative positions of the polymer T_1 and CT states constrain V_{OC} (without J_{SC} loss) in organic photovoltaics.[20] While strong evidence for substantial recombination losses via the polymer T_1 state have indeed been observed in many high V_{OC} systems,[7,13−16,19,20,22] our data suggest that the position of the polymer T_1 state need not limit J_{SC} in organic solar cells. Apparently, kinetics can permit efficient charge separation in some systems even when a thermodynamically favorable recombination pathway exists.

Next, we use photoinduced absorption (PIA) spectroscopy to probe the long-lived excited states that are formed following photoexcitation of PIDT-PhanQ blends with different fullerenes. PIA is a pump−probe technique measuring changes in optical transmission (ΔT) due to formation of long-lived excited states (e.g., polarons or triplets with lifetimes on the order of $\tau \sim \mu s - ms$).[7,30,31,61−64] Assuming there are no changes in reflection, normalized differential transmission ($\Delta T/T$) may be plotted in terms of the differential absorption coefficient $\Delta\alpha d = -\ln[1+\Delta T/T]$ (d being film thickness). Figure 3a shows the PIA spectra for neat PIDT-PhanQ at room temperature (dashed red trace) and at 80K (red filled circles), and for $IC_{60}BA$ dispersed in polystyrene at room temperature (dashed black trace) and at 80K (black unfilled circles). As expected, the room temperature spectra of the pure components show almost no PIA signal: very few polarons are formed in a pure polymer, and at room temperature the triplet lifetime is too short to accumulate a significant population. The PIA spectrum at 80K consists primarily of triplet−triplet absorption in the $IC_{60}BA$ film. This fullerene triplet spectrum is consistent with triplet absorption spectra for other C_{60} derivatives reported in the literature.[65] However, the PIDT-PhanQ PIA spectrum at 80K is broad and structured, with a peak near λ = 1100 nm and a shoulder tailing out to λ = 1400 nm. As we show in Figure 3b, the PIDT-PhanQ PIA features at 1400 nm (gray shaded region labeled T_1 in Figure 3a and unfilled circles label T_1 in Figure 3b) exhibit a weaker dependence on modulation frequency than the PIDT-PhanQ PIA peak near 1100 nm (gray shaded region labeled P+ in Figure 3a and red filled circles labeled P+ in Figure 3b). This difference in modulation frequency dependence is consistent with our assignment of the peaks to separate species. As we discuss below, we assign the PIDT-PhanQ photoinduced absorption in the 1400 nm T_1 region to PIDT-PhanQ triplet excitons based on their modulation dependence, temperature dependence, and spectral line shape (cf. Supporting Information Figure S3 and Figure S4).

Figure 3c shows PIA spectra measured at room temperature for PIDT-PhanQ blended with $PC_{61}BM$ or $IC_{60}BA$. Compared to the pure polymer film, the PIDT-PhanQ:$PC_{61}BM$ blend (black dashed trace in Figure 3c) exhibits a distinct peak (gray region labeled P+) centered at 1070 nm that has a different line shape and modulation dependence from the triplet peak observed in the pure polymer. We observe an identical PIA peak at 1070 nm (Supporting Information Figure S4) when PIDT-PhanQ is blended with fullerenes **5**, **6**, *bis*-$PC_{61}BM$, or $PC_{71}BM$. Although anion absorption for C_{60} derivatives typically occurs between 1000 and 1100 nm depending on functionalization,[66] we assign this 1070 nm feature as the

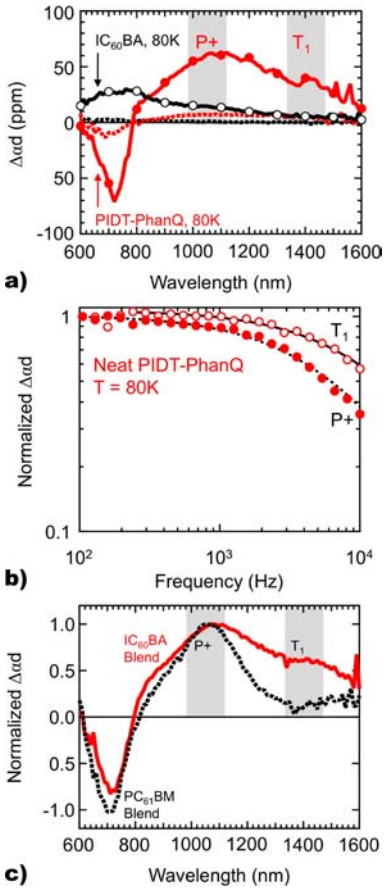

Figure 3. (a) Photoinduced absorption (PIA) spectra of isolated PIDT-PhanQ at T = 80 K (filled red circles) overlaid with that for $IC_{60}BA$ (unfilled black circles). Spectra acquired at room temperature are also included (dashed red trace = neat polymer, dashed black trace = fullerene). (b) PIA Modulation frequency dependence for neat PIDT-PhanQ measured in the T_1 and P+ spectral regions shown in Figure 3a. Data measured at T = 80K. Black lines represent dispersive fits to the data described in Supporting Information. (c) Normalized PIA spectra of PIDT-PhanQ:fullerene blends collected at room temperature showing PIDT-PhanQ polaron absorption (P+) at 1070 nm when blended with $PC_{61}BM$ (dashed black trace) and PIDT-PhanQ triplet (T_1) absorption when blended with $IC_{60}BA$ (solid red trace). The gray regions labeled T_1 and P+ signify the spectral positions of the polymer triplet and the positive polymer polaron, respectively. Note: PIA features corresponding to anion formation on the fullerene C_{60} cage typically occur at ca. 1100 nm. However, we are unable to resolve this feature in these particular blends, due to overlap with the polymer cation (P+).

absorption of the polymer polaron, both because the fullerene anion absorption is typically weaker than the polymer absorption by a factor of 10, and because the 1070 nm peak occurs at the identical position and shape for all (except ICBA) of the fullerenes we have studied, including $PC_{71}BM$, where the anion absorption is known to occur at 1350 nm.[67] In agreement with this assignment, we observe a light-induced electron paramagnetic resonance (LEPR) spectrum for PIDT-PhanQ:$PC_{61}BM$ that is consistent with photoinduced polaron formation (dashed black trace in Supporting Information Figure S11).

In contrast, the PIA spectrum of the $IC_{60}BA$ blend at room temperature (solid red trace in Figure 3c) shows a line shape different from that observed for polaron formation in PIDT-PhanQ:$PC_{61}BM$ and all other PIDT-PhanQ:fullerene blends that we have examined (Supporting Information Figure S4). In addition, the modulation dependence of the blend spectra (Supporting Information Figure S3b) indicate that the species observed in the ICBA blend is much shorter-lived than the polaron signature observed in the PCBM blend. Indeed, the room temperature $IC_{60}BA$ blend PIA spectrum (Figure 3c) overlays the pristine polymer spectrum collected at 80 K (Figure 3a), showing a peak at 1400 nm. We thus assign this feature in the ICBA blend to the PIDT-PhanQ polymer triplet absorption. In support of this assignment, we also observe stronger temperature dependence for this T_1 feature compared to the P+ polaron feature in our PIDT-PhanQ:$PC_{61}BM$ blends (cf. Supporting Information Figure S4c and S4d).

Taken together, the photoluminescence and PIA data indicate that the polymer singlet excitons are completely quenched in all of the PIDT-PhanQ:fullerene blends and that in blends of the polymer with any fullerene except ICBA the primary species observed at room temperature are polymer polarons. In contrast, we observe a high density of polymer triplets in PIDT-PhanQ:ICBA blends at room temperature. These data suggest that polymer triplets are efficiently formed in the PIDT-PhanQ:ICBA blend, likely as a result of polaron pair recombination, as observed in numerous donor/acceptor systems.[7,15,19,20,22] Since the CT state at the D/A interface in our systems lies 300 meV or more above the polymer triplet energy for all of the studied blends, we believe it is unlikely that the small increase in reduction potential of the fullerene in moving from fullerene **6** to ICBA (a change in reduction potential of only ca. −20 mV) would be sufficient to turn on recombination directly from the CT state to the polymer triplet in the ICBA blend but not in the other blends.

Instead, Figure 4a presents a proposed energy level diagram and recombination scheme that is consistent with all of our experimental data. Quenching of the S_1 states of the polymer (1.61 eV) or the fullerene (1.69 eV) leads to either free charges or population of the lowest energy charge transfer state (CT_1 = 1.44 eV), which is nearly degenerate with the ICBA T_1 state at 1.48 eV. We propose that the fullerene triplet state may serve as an important intermediate in the recombination process in PIDT-PhanQ:$IC_{60}BA$ blends and may decay either by Dexter energy transfer to the polymer T_1 state (1.01 eV), or by direct decay (both radiative and nonradiative) to the fullerene ground state. We therefore return to consider the PL spectra in Figure 2b in more detail. We noted earlier that the PL spectrum for the PIDT-PhanQ:ICBA blend exhibited structure that was inconsistent with CT state emission. We propose that this structured emission band instead represents fullerene phosphorescence, since the peak energy is consistent with reported triplet emission for C_{60} derivatives.[48,68−72]

To test this hypothesis, we measured heavy-atom-sensitized $IC_{60}BA$ phosphorescence at T = 80 K. Figure 4b shows the sensitized ICBA phosphorescence obtained in ethyliodide:2-methyltetrahydrofuran (C_2H_5I:MeTHF, 50:50 by volume) overlaid with the low-temperature PL from the PIDT-PhanQ:ICBA blend. From the similarity between the sensitized phosphorescence (T_1 peaks at 840 and 955 nm) and the blend PL in the spectral region between 800 and 1000 nm we conclude that the unusual blend PL signal is triplet emission from the ICBA. We note that the blend phosphorescence is surprisingly intense: it is brighter than the unstructured CT state emission of the other polymer:fullerene blends. Indeed, under similar conditions, the $IC_{60}BA$ phosphorescence in the blend is at least six times more intense than that of the

dx.doi.org/10.1021/ja306110b | J. Am. Chem. Soc. 2012, 134, 19661−19668

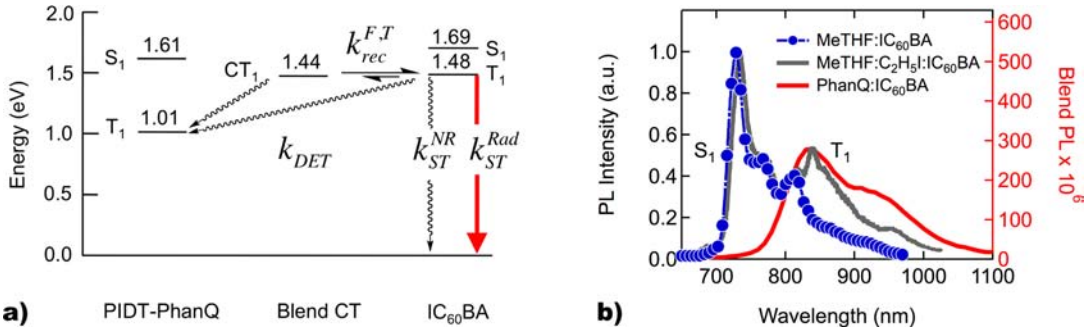

Figure 4. (a) State energies and proposed recombination pathways for PIDT-PhanQ:$IC_{60}BA$ charge recombination from the charge transfer state (CT_1) to the triplet state (T_1) of either the polymer or the fullerene, and fullerene triplet generation occurring via this route with rate constant $k_{rec}^{F,T}$. Decay from the fullerene T_1 state may occur via phosphorescence with rate constant k_{ST}^{Rad}, Dexter excitation transfer to the polymer T_1 state with rate constant k_{DET}, and nonradiative relaxation with rate constant k_{ST}^{NR}. The CT_1 energy for the blend was determined using the correlation between PL peak maximum and reduction potential in Figure 2d, the upper limit for the polymer T_1 was estimated relative to the S_1 peak maximum based on quantum chemical calculations and recognizing common empirical singlet−triplet splittings of ΔE_{ST} = 0.60−0.75 eV[57−60] for many reported conjugated polymers. The fullerene T_1 energy was determined using the phosphorescence peak in (b). (b) PL spectra for $IC_{60}BA$ in frozen 2-methyltetrahydrofuran (MeTHF) in the presence (solid gray trace = phosphorescence + fluorescence) and absence (filled blue circles = fluorescence) of C_2H_5I are overlaid with the PIDT-PhanQ:$IC_{60}BA$ blend PL (solid red trace), all measured at 80 K.

fluorescence signal observed from an $IC_{60}BA$:polystyrene film of comparable optical density (Supporting Information Figure S5), suggesting that the fullerene triplet state is populated more rapidly in the blend than by native singlet-to-triplet intersystem crossing on the fullerene alone. Previous studies have shown that changes in film morphology can affect the ratio of polarons to triplets produced in blended donor:acceptor films.[73−75] While we cannot exclude the possibility that the low FF in our ICBA devices may be due to differences in morphology, we can exclude morphological coarsening as the cause of the increased triplet population observed in the ICBA blend. In previous work focused on controlling morphology of PIDT-PhanQ:fullerene blends[76] we observed no increase in triplet generation as the length scale of phase separation was tuned from ∼20 nm to ∼1 μm with solvent additives. This observation suggests that the origin of the increased triplet yield is not inherently morphological in character.

We conclude that the increased polymer triplet yield observed in the PIA spectroscopy of the PIDT-PhanQ:ICBA blend is the result of Dexter energy transfer from the fullerene triplet to the polymer triplet. The CT_1 state in this blend is nearly degenerate with the fullerene T_1 state (consistent with the $IC_{60}BA$ phosphorescence observed in the blend), but below the S_1 states of the polymer and the fullerene (fluorescence quenched in the blend). Given the observed phosphorescence from the polymer:ICBA blend, and the rapid nonradiative decay of fullerene triplets, it is likely that only a fraction of the triplets undergo energy transfer to the polymer. Nevertheless, this population is much higher than the triplet population encountered in a pristine polymer.

The lower IQE in our ICBA devices could be due to a number of factors. For example, in theory, a decrease in the dissociation rate of bound CT states into polarons or an increase in CT state recombination rate could account for a drop in IQE (cf. Supporting Information Figure S12). However, recent results suggest that rapid charge separation leading to efficient photocurrent collection appears to proceed through higher lying CT states.[77] In the latter case, the IQE is dictated by the rate at which the system reaches delocalized charge separated states relative to the formation rate of localized CT states at the D/A interface. Similarly, we believe that in certain systems low-lying triplet states need not limit efficient photocurrent collection in organic solar cells (e.g., PIDT-PhanQ:PCBM), since the process of charge separation may kinetically outcompete other loss processes. Additionally, anomalously high triplet populations may not always form most rapidly via the lowest energy triplet state, but rather through other higher-lying triplet states that may be more kinetically accessible (e.g., PIDT-PhanQ:ICBA). Our results demonstrate the importance of (1) reevaluating the mechanisms by which free charges, bound CT states, and triplets are formed and (2) understanding how these processes influence design principles for rational optimization of organic semiconducting materials.

■ CONCLUSIONS

In summary, we observe internal quantum efficiencies of up to 95% in polymer:fullerene blend solar cells for which the driving force for direct recombination from the relaxed CT_1 state to the polymer triplet state is ∼300 meV. This result is in contrast to both intuition and successful empirical guidelines[7,15,19−23] for device optimization that suggest recombination should proceed through the polymer triplet state under such circumstances. On the other hand, as the charge transfer state energy is raised via fullerene derivatization, we do observe evidence for large triplet populations on both the polymer and fullerene, but only after the energy of the charge transfer state is raised close to the energy of the fullerene T_1, indicating that the fullerene is the gateway to the triplet species we observe at room temperature in the photoinduced absorption spectroscopy for this blend. It is unclear if the increased triplet population in the ICBA blend is the cause, or merely a symptom, of the failings of this blend. Nevertheless, we find the correlation an interesting one that may warrant study in the future.

We believe these observations are compatible with reports that charge separation occurs primarily from higher lying "hot" CT states.[77] In that scenario, the escape of charge carriers from the donor/acceptor interface would predominantly occur prior to localization into the relaxed CT state, making the energy of the cooled CT state relative to the polymer triplet less important than the kinetics of carrier escape from the D/A interface relative to those of cooling to the relaxed CT state. Increased triplet yields would then result either from bimolecular recombination of photogenerated carriers, or from relaxation of a cooled CT state (geminate or bimolecular),

dx.doi.org/10.1021/ja306110b | J. Am. Chem. Soc. 2012, 134, 19661−19668

via the most kinetically accessible triplet state. While our results suggest that nearly 100% internal quantum efficiency can be achieved in OPV systems where photocurrent collection can kinetically outcompete recombination via low-lying polymer triplet excitons, we note that we do expect bimolecular recombination via polymer triplet states under a resistive load, where charge carriers are not extracted quickly or at open circuit.

These results suggest two important considerations for the optimization of organic solar cells. First, as noted before, the fullerene triplet can serve as an important recombination intermediate, especially in blends where a substantial portion of the light is absorbed by the fullerene.[14,16,78] Second, and more importantly, photocurrent losses via triplet states may be avoided kinetically as a result of either slow triplet formation or fast carrier escape from the interface. We speculate that kinetic strategies such as modulating local dipole moments, tailoring dielectric constants, optimizing interfacial electronic coupling, and controlling reorganization energies might be fruitful approaches to overcome losses when attempting to maintain high photocurrents in high V_{OC} organic solar cells.

■ ASSOCIATED CONTENT

Supporting Information

Additional spectra (calculated absorption, PIA, PL, and LEPR), PIA frequency modulation and temperature dependence, AFM surface topography images, quantum chemical computational results and methods. This material is available free of charge via the Internet at http://pubs.acs.org.

■ AUTHOR INFORMATION

Corresponding Author

ginger@chem.washington.edu

Present Address

[§]Laboratory for Neutron Scattering, Paul Scherrer Institut, CH-5232 Villigen PSI, Switzerland

Notes

The authors declare no competing financial interest.

■ ACKNOWLEDGMENTS

This paper is based on work supported primarily by the ONR (thin film spectroscopy and analysis by C.W.S. and D.S.G., materials development and characterization by A.K.Y.J., N00014-11-1-0300). C.W.S. acknowledges partial support from the US NSF SEES fellowship program (analysis, GEO-1215753). We acknowledge additional support from the AOARD for K.S.C. (device fabrication and testing, FA2386-11-1-4072) and the World Class University program through the National Research Foundation of Korea under the Ministry of Education, Science and Technology (R31-21410035). X.S.L. and F.Z.D. acknowledge US NSF CHE-CAREER 0844999 for support of the triplet energy level calculations. D.R.G., L.R.B., and S.T.O. acknowledge US NSF CHE-1213283 for support of EPR and solution PL measurements and analysis. A portion was conducted using the facilities at the UW NanoTech User Facility, a member of the NSF National Nanotechnology Infrastructure Network. We thank Jingyu Zou for ellipsometric measurements, José Francisco Salinas Torres for helpful discussion regarding optical modeling, and Dr. Xinghua Zhou for PIDT-PhanQ synthesis.

■ REFERENCES

(1) He, Z.; Zhong, C.; Huang, X.; Wong, W.-Y.; Wu, H.; Chen, L.; Su, S.; Cao, Y. *Adv. Mater.* **2011**, *23*, 4636−4643.
(2) Green, M. A.; Emery, K.; Hishikawa, Y.; Warta, W. *Prog. Photovoltaics* **2010**, *18*, 346−352.
(3) Liang, Y. Y.; Xu, Z.; Xia, J. B.; Tsai, S. T.; Wu, Y.; Li, G.; Ray, C.; Yu, L. P. *Adv. Mater.* **2010**, *22*, E135−E138.
(4) Kromhout, W. W. *UCLA engineers create tandem polymer solar cells that set record for energy-conversion*; UCLA Newsroom: Los Angeles, CA, 2012.
(5) Servaites, J. D.; Ratner, M. A.; Marks, T. J. *Appl. Phys. Lett.* **2009**, 95.
(6) Servaites, J. D.; Ratner, M. A.; Marks, T. J. *Energ. Environ. Sci.* **2011**, *4*, 4410−4422.
(7) Veldman, D.; Meskers, S. C. J.; Janssen, R. A. J. *Adv. Funct. Mater.* **2009**, *19*, 1939−1948.
(8) Faist, M. A.; Kirchartz, T.; Gong, W.; Ashraf, R. S.; McCulloch, I.; de Mello, J. C.; Ekins-Daukes, N. J.; Bradley, D. D. C.; Nelson, J. *J. Am. Chem. Soc.* **2012**, *134*, 685−692.
(9) Vandewal, K.; Tvingstedt, K.; Gadisa, A.; Inganas, O.; Manca, J. V. *Nat. Mater.* **2009**, *8*, 904−909.
(10) Vandewal, K.; Tvingstedt, K.; Gadisa, A.; Inganas, O.; Manca, J. V. *Phys. Rev. B* **2010**, *81*, 125204.
(11) Rand, B. P.; Burk, D. P.; Forrest, S. R. *Phys. Rev. B* **2007**, *75*, 115327.
(12) Mutolo, K. L.; Mayo, E. I.; Rand, B. P.; Forrest, S. R.; Thompson, M. E. *J. Am. Chem. Soc.* **2006**, *128*, 8108−8109.
(13) Ohkita, H.; Cook, S.; Astuti, Y.; Duffy, W.; Tierney, S.; Zhang, W.; Heeney, M.; McCulloch, I.; Nelson, J.; Bradley, D. D. C.; Durrant, J. R. *J. Am. Chem. Soc.* **2008**, *130*, 3030−3042.
(14) Benson-Smith, J. J.; Ohkita, H.; Cook, S.; Durrant, J. R.; Bradley, D. D. C.; Nelson, J. *Dalton Trans.* **2009**, 10000−10005.
(15) Westenhoff, S.; Howard, I. A.; Hodgkiss, J. M.; Kirov, K. R.; Bronstein, H. A.; Williams, C. K.; Greenham, N. C.; Friend, R. H. *J. Am. Chem. Soc.* **2008**, *130*, 13653−13658.
(16) Ohkita, H.; Cook, S.; Astuti, Y.; Duffy, W.; Heeney, M.; Tierney, S.; McCulloch, I.; Bradley, D. D. C.; Durrant, J. R. *Chem. Commun.* **2006**, 3939−3941.
(17) Deibel, C.; Strobel, T.; Dyakonov, V. *Adv. Mater.* **2010**, *22*, 4097−4111.
(18) Giebink, N. C.; Wiederrecht, G. P.; Wasielewski, M. R.; Forrest, S. R. *Phys. Rev. B* **2010**, *82*, 155305.
(19) Giebink, N. C.; Lassiter, B. E.; Wiederrecht, G. P.; Wasielewski, M. R.; Forrest, S. R. *Phys. Rev. B* **2010**, *82*, 155306.
(20) Liedtke, M.; Sperlich, A.; Kraus, H.; Baumann, A.; Deibel, C.; Wirix, M. J. M.; Loos, J.; Cardona, C. M.; Dyakonov, V. *J. Am. Chem. Soc.* **2011**, *133*, 9088−9094.
(21) Koster, L. J. A.; Shaheen, S. E.; Hummelen, J. C. *Adv. Energy Mater.* **2012**, *2*, 1246−1253.
(22) Veldman, D.; Ipek, O.; Meskers, S. C. J.; Sweelssen, J.; Koetse, M. M.; Veenstra, S. C.; Kroon, J. M.; van Bavel, S. S.; Loos, J.; Janssen, R. A. J. *J. Am. Chem. Soc.* **2008**, *130*, 7721−7735.
(23) Dutton, G. J.; Jin, W.; Reutt-Robey, J. E.; Robey, S. W. *Phys. Rev. B* **2010**, *82*, 073407.
(24) He, Y.; Chen, H.-Y.; Hou, J.; Li, Y. *J. Am. Chem. Soc.* **2010**, *132*, 1377−1382.
(25) He, Y.; Zhao, G.; Peng, B.; Li, Y. *Adv. Funct. Mater.* **2010**, *20*, 3383−3389.
(26) Laird, D. W.; Stegamat, R.; Richter, H.; Vejins, V.; Scott, L.; Lada, T. A. Organic photovoltaic devices comprising fullerenes and derivatives thereof, US Patent 8217260, 2008.
(27) Li, C.-Z.; Yip, H.-L.; Jen, A. K.-Y. *J. Mater. Chem.* **2012**, *22*, 4161−4177.
(28) Li, C.-Z.; Chien, S.-C.; Yip, H.-L.; Chueh, C.-C.; Chen, F.-C.; Matsuo, Y.; Nakamura, E.; Jen, A. K.-Y. *Chem. Commun.* **2011**, *47*, 10082−10084.
(29) Zhang, Y.; Zou, J.; Yip, H.-L.; Chen, K.-S.; Zeigler, D. F.; Sun, Y.; Jen, A. K.-Y. *Chem. Mater.* **2011**, *23*, 2289−2291.

(30) Noone, K. M.; Anderson, N. C.; Horwitz, N. E.; Munro, A. M.; Kulkarni, A. P.; Ginger, D. S. *ACS Nano* **2009**, *3*, 1345−1352.
(31) Ginger, D. S.; Greenham, N. C. *Phys. Rev. B* **1999**, *59*, 10622−10629.
(32) Burkhard, G. F.; Hoke, E. T.; McGehee, M. D. *Adv. Mater.* **2010**, *22*, 3293−3297.
(33) Hwang, J.; Wan, A.; Kahn, A. *Mater. Sci. Eng., R* **2009**, *64*, 1−31.
(34) Yu, C.-Y.; Chen, C.-P.; Chan, S.-H.; Hwang, G.-W.; Ting, C. *Chem. Mater.* **2009**, *21*, 3262−3269.
(35) Pina, J.; de Melo, J. S.; Burrows, H. D.; Bunnagel, T. W.; Dolfen, D.; Kudla, C. J.; Scherf, U. *J. Phys. Chem. B* **2009**, *113*, 15928−15936.
(36) Chen, C.-P.; Chan, S.-H.; Chao, T.-C.; Ting, C.; Ko, B.-T. *J. Am. Chem. Soc.* **2008**, *130*, 12828−12833.
(37) Zhang, W.; Smith, J.; Watkins, S. E.; Gysel, R.; McGehee, M.; Salleo, A.; Kirkpatrick, J.; Ashraf, S.; Anthopoulos, T.; Heeney, M.; McCulloch, I. *J. Am. Chem. Soc.* **2010**, *132*, 11437−11439.
(38) Schroeder, B. C.; Huang, Z.; Ashraf, R. S.; Smith, J.; D'Angelo, P.; Watkins, S. E.; Anthopoulos, T. D.; Durrant, J. R.; McCulloch, I. *Adv. Funct. Mater.* **2012**, *22*, 1663−1670.
(39) McCulloch, I.; Ashraf, R. S.; Biniek, L.; Bronstein, H.; Combe, C.; Donaghey, J. E.; James, D. I.; Nielsen, C. B.; Schroeder, B. C.; Zhang, W. *Acc. Chem. Res.* **2012**, *45*, 714−722.
(40) Bronstein, H.; Leem, D. S.; Hamilton, R.; Woebkenberg, P.; King, S.; Zhang, W.; Ashraf, R. S.; Heeney, M.; Anthopoulos, T. D.; de Mello, J.; McCulloch, I. *Macromolecules* **2011**, *44*, 6649−6652.
(41) Chen, K.-S.; Zhang, Y.; Yip, H.-L.; Sun, Y.; Davies, J. A.; Ting, C.; Chen, C.-P.; Jen, A. K.-Y. *Org. Electron.* **2011**, *12*, 794−801.
(42) Hoke, E. T.; Vandewal, K.; Bartelt, J. A.; Mateker, W. R.; Douglas, J. D.; Noriega, R.; Graham, K. R.; Fréchet, J. M. J.; Salleo, A.; McGehee, M. D. *Adv. Energy Mater.* **2012**, DOI: 10.1002/aenm.201200474.
(43) Di Nuzzo, D.; Wetzelaer, G.-J. A. H.; Bouwer, R. K. M.; Gevaerts, V. S.; Meskers, S. C. J.; Hummelen, J. C.; Blom, P. W. M.; Janssen, R. A. J. *Adv. Energy Mater.* **2012**, DOI: 10.1002/aenm.201200426.
(44) Miller, N. C.; Sweetnam, S.; Hoke, E. T.; Gysel, R.; Miller, C. E.; Bartelt, J. A.; Xie, X.; Toney, M. F.; McGehee, M. D. *Nano Lett.* **2012**, *12*, 1566−1570.
(45) Park, S. H.; Roy, A.; Beaupre, S.; Cho, S.; Coates, N.; Moon, J. S.; Moses, D.; Leclerc, M.; Lee, K.; Heeger, A. J. *Nat. Photonics* **2009**, *3*, 297−U5.
(46) Chen, H.-Y.; Hou, J.; Zhang, S.; Liang, Y.; Yang, G.; Yang, Y.; Yu, L.; Wu, Y.; Li, G. *Nat. Photonics* **2009**, *3*, 649−653.
(47) Thomas, K. G.; Biju, V.; George, M. V.; Guldi, D. M.; Kamat, P. V. *J. Phys. Chem. A* **1998**, *102*, 5341−5348.
(48) Williams, R. M.; Zwier, J. M.; Verhoeven, J. W. *J. Am. Chem. Soc.* **1995**, *117*, 4093−4099.
(49) Gould, I. R.; Noukakis, D.; Gomezjahn, L.; Young, R. H.; Goodman, J. L.; Farid, S. *Chem. Phys.* **1993**, *176*, 439−456.
(50) Gould, I. R.; Young, R. H.; Moody, R. E.; Farid, S. *J. Phys. Chem.* **1991**, *95*, 2068−2080.
(51) Kim, H.; Kim, J. Y.; Park, S. H.; Lee, K.; Jin, Y.; Kim, J.; Suh, H. *Appl. Phys. Lett.* **2005**, *86*, 183502.
(52) Morteani, A. C.; Sreearunothai, P.; Herz, L. M.; Friend, R. H.; Silva, C. *Phys. Rev. Lett.* **2004**, *92*, 247402.
(53) Tvingstedt, K.; Vandewal, K.; Gadisa, A.; Zhang, F. L.; Manca, J.; Inganas, O. *J. Am. Chem. Soc.* **2009**, *131*, 11819−11824.
(54) Loi, M. A.; Toffanin, S.; Muccini, M.; Forster, M.; Scherf, U.; Scharber, M. *Adv. Funct. Mater.* **2007**, *17*, 2111−2116.
(55) Ng, A. M. C.; Djurisic, A. B.; Chan, W. K.; Nunzi, J. M. *Chem. Phys. Lett.* **2009**, *474*, 141−145.
(56) We note that assigning state energies based on the spectral onset of absorption and emission bands yields a qualitatively equivalent ordering of energy states, leading to similar conclusions.
(57) Kohler, A.; Wilson, J. S.; Friend, R. H.; Al-Suti, M. K.; Khan, M. S.; Gerhard, A.; Bassler, H. *J. Chem. Phys.* **2002**, *116*, 9457−9463.
(58) Kohler, A.; Beljonne, D. *Adv. Funct. Mater.* **2004**, *14*, 11−18.
(59) Hertel, D.; Setayesh, S.; Nothofer, H. G.; Scherf, U.; Mullen, K.; Bassler, H. *Adv. Mater.* **2001**, *13*, 65−70.
(60) Monkman, A. P.; Burrows, H. D.; Hartwell, L. J.; Horsburgh, L. E.; Hamblett, I.; Navaratnam, S. *Phys. Rev. Lett.* **2001**, *86*, 1358−1361.
(61) Korovyanko, O. J.; Osterbacka, R.; Jiang, X. M.; Vardeny, Z. V.; Janssen, R. A. J. *Phys. Rev. B* **2001**, *64*, 235122.
(62) Janssen, R. A. J.; Christiaans, M. P. T.; Hare, C.; Martin, N.; Sariciftci, N. S.; Heeger, A. J.; Wudl, F. *J. Chem. Phys.* **1995**, *103*, 8840−8845.
(63) Noone, K. M.; Strein, E.; Anderson, N. C.; Wu, P.-T.; Jenekhe, S. A.; Ginger, D. S. *Nano Lett.* **2010**, *10*, 2635−2639.
(64) Noone, K. M.; Subramaniyan, S.; Zhang, Q.; Cao, G.; Jenekhe, S. A.; Ginger, D. S. *J. Phys. Chem. C* **2011**, *115*, 24403−24410.
(65) Bensasson, R. V.; Bienvenue, E.; Fabre, C.; Janot, J. M.; Land, E. J.; Leach, S.; Leboulaire, V.; Rassat, A.; Roux, S.; Seta, P. *Chem.—Eur. J.* **1998**, *4*, 270−278.
(66) Guldi, D. M.; Prato, M. *Acc. Chem. Res.* **2000**, *33*, 695−703.
(67) Sperlich, A.; Liedtke, M.; Kern, J.; Kraus, H.; Deibel, C.; Filippone, S.; Luis Delgado, J.; Martin, N.; Dyakonov, V. *Phys. Stat. Sol.-Rapid Res. Lett.* **2011**, *5*, 128−130.
(68) Sassara, A.; Zerza, G.; Chergui, M. *Chem. Phys. Lett.* **1996**, *261*, 213−220.
(69) Vandenheuvel, D. J.; Chan, I. Y.; Groenen, E. J. J.; Schmidt, J.; Meijer, G. *Chem. Phys. Lett.* **1994**, *231*, 111−118.
(70) Prat, F.; Marti, C.; Nonell, S.; Zhang, X. J.; Foote, C. S.; Moreno, R. G.; Bourdelande, J. L.; Font, J. *Phys. Chem. Chem. Phys.* **2001**, *3*, 1638−1643.
(71) Guldi, D. M.; Asmus, K. D. *J. Phys. Chem. A* **1997**, *101*, 1472−1481.
(72) Luo, C.; Fujitsuka, M.; Watanabe, A.; Ito, O.; Gan, L.; Huang, Y.; Huang, C. H. *J. Chem. Soc., Faraday Trans.* **1998**, *94*, 527−532.
(73) Di Nuzzo, D.; Aguirre, A.; Shahid, M.; Gevaerts, V. S.; Meskers, S. C. J.; Janssen, R. A. J. *Adv. Mater.* **2010**, *22*, 4321−4324.
(74) Snedden, E. W.; Monkman, A. P.; Dias, F. B. *J. Phys. Chem. C* **2012**, *116*, 4390−4398.
(75) Tvingstedt, K.; Vandewal, K.; Zhang, F.; Inganas, O. *J. Phys. Chem. C* **2010**, *114*, 21824−21832.
(76) Chen, K.-S.; Yip, H.-L.; Schlenker, C. W.; Ginger, D. S.; Jen, A. K.-Y. *Org. Electron.* **2012**, *13*, 2870−2878.
(77) Bakulin, A. A.; Rao, A.; Pavelyev, V. G.; van Loosdrecht, P. H. M.; Pshenichnikov, M. S.; Niedzialek, D.; Cornil, J.; Beljonne, D.; Friend, R. H. *Science* **2012**, *335*, 1340−1344.
(78) Cook, S.; Ohkita, H.; Durrant, J. R.; Kim, Y.; Benson-Smith, J. J.; Nelson, J.; Bradley, D. D. C. *Appl. Phys. Lett.* **2006**, *89*, 101128.